Stator Inter-turn Fault Detection in Inverter Fed InductionMotor Drives

Ms. S. Kamatchi, Ms. B. Thamizhkani[2] , Mr.S.Nagarajan@vengateshkumar[3]
Department of Electrical and Electronics Engineering
Dhanalakshmi Srinivasan College of Engineering and Technology

ABSTRACT

The Squirrel Cage Induction Motor (SCIM) with advanced power electronic inverters presents the greater advantages on cost and energy efficiency as compared with other industrial solutions for varying speed applications. In recent, the inverter fed induction motors are being popular in the industries. These inverter fed-motors are recently gathering great recognition for multi- megawatt industrial drive applications. In this present paper, a dynamic simulation model of PWM inverter fed SCIM with direct torque control jointly has been presented and analyzed in the recent MATLAB/Simulink environment. From the proposed simulation model, the transient behavior of SCIM has been analysed for healthy as well as for stator inter-turn fault condition. The dynamic simulation of induction motor is one of the key steps in the validation of design process of the electric motor and drive system. It is extremely needed for eliminating probable faults beforehand due to inadvertent design mistakes and changes during operation. The simulated model gives encouraging results with reduced harmonics [1]. By using the model, the successful detection of stator inter-turn fault of the SCIM is carried out in the transient condition. Therefore, early stator fault detection is possible and may avoid the motor to reach in the catastrophic conditions. Therefore, may save millions of dollars for industries

Keyword:

Induction MOTOR Modelling and simulationPulse Width Modulation Stator fault
Time Domain Analysis

.

1. INTRODUCTION

Nowadays, the Induction Motor (IM) with Pulse Width Modulation (PWM) inverters drives are widely used in many variable speed industrial applications and replacing DC motor and thyrister bridges. Therefore, in the present time, it is highly essential to develop models with the help of recent software which may detect IM faults as early as possible. If any fault occurs and not diagnosed timely then the failure of the electric motor can cause substantial financial losses and even damage of the whole drive system [1-3].

A comprehensive review of health monitoring and fault diagnosis techniques can be found in [2]. It has been observed that the stator faults are responsible for 37% of the IM failures and, after the bearing faults, are the most recurrent reasons of the IM damages.

The stator current and vibrations are extensively used for many induction motor fault diagnoses purpose. Due to ease of measurements, the stator current signals are most widely used for this purpose and thus different analysis methods have been developed, based on detection of sidebands harmonics at certain frequencies. Such methods like Fast Fourier Transform (FFT), Short Time Fourier Transform (STFT), and the Wavelet Transform (WT) [2-8].

Among the total induction motor faults, around 30-40 % are related to the stator

winding insulation and core. It can also be seen that a large portion of stator winding-related faults are initiated by insulation failures in several turns of a stator coil within one phase [9-10]. Among the possible causes, thermal stresses are the main reason for the degradation of the stator winding insulation. Generally, stator winding insulation thermal stresses are categorized into three types: aging, overloading and cycling [9]. The contamination ofthe insulating materials used in the induction machines, combination of thermal overloading and cycling, transient voltage stresses, mechanical stresses etc. are the other possible reasons for the deterioration of the insulation. Electrical stresses, mainly related to the machine terminal voltages, also cause insulation degradation. Among the various electrical stresses, partial discharges (PDs) in the windings and transient voltages at the machine terminals are considered as the major contributors [11].

With the increased emphasis on energy conservation and high performance motor control, the use of Pulse Width-Modulated Voltage Source Inverters (PWM-VSIs) has grown at an exponential rate. This has made the stator windings open to higher electrical stresses. High speed PWM operations introduce high rate of rise of transient voltages at the machine terminals. Current in the stator winding produces a force on the coils that is proportional to the square of the current. This force is at its maximum under transient overloads, causing the coils to vibrate at twice the synchronous frequency with movement in both the radial and the tangential direction. This movement weakens the integrity of the insulation system. Contaminations due to foreign materials can lead to adverse effects on the stator winding insulation [1], [10], [12].

Stator winding-related failures can be broadly classified into the following four groups: open-circuit faults, turn-to-turn, line-to-ground, line-to-line, and single or multi-phase winding. Among these four failure modes, turn-to-turn faults (stator turn faults) have been considered as the most challenging one since the other types of failures are usually the consequences of turn faults. It can be seen that among the faults, the inter turn faults are the most difficult fault to detect at an early stage itself. To solve the difficulty in detecting turn faults, several methods have been suggested [13-20]. Because of this, remarkable improvements have been achieved in the area of stator turn fault detection. Nevertheless, the question about the delay time between a turn fault and other severe failures still remains to be answered.

The internal asymmetry due to inter turn fault will cause the circulation of extremely high currents in the portion of the winding affected by the fault, thus contributing to the degradation of other portions of the windings. The lead time between the start of the fault and the complete failure of the machine depends on several factors, namely the initial number of shorted turns, winding configuration, rated power, rated voltage,environmental condition etc [9].

If the fault can be predicted at an early stage, a catastrophic effect can be avoided, the machine can be protected as well as the safety of the working personnel shall be ensured. In the case of a stator turn fault, a large circulating current will be produced, leading to excessive heat generation in the shorted turns. The heat, which is proportional to the square of the circulating current, accelerates the severity of the fault to a destructive level [18]. If this fault is not detected at the early stage it will be propagated and will lead to phase to ground or phase-to-phase fault which in turn may lead to the damage of the machine. As the inter turn fault is one of the major reasons for the machine failure. Intensive investigations on stator turn faults revealed that the faults introduce specific changes in the electric properties of the machines. This has created a great dealof scope to develop methods for the detection of a turn fault [13], [15], [19].

In the present paper, a PWM inverter fed Induction Motor model has been proposed and diagnosed stator inter-turn fault in the transient conditions. By this model, many researchers in future may diagnose various IM faults in the transient conditions by various

advanced Digital Signal Processing Techniques such as FFT and wavelet Transofrm.

2. MATHEMATICAL MODELLING OF HEALTHY AND FAULTY CONDITIONS OF THE IM

The mathematical modelling of the induction motor for healthy and faulty motor has been discussedin the next section step by step.

Modelling of healthy condition of the motor

The mathematical modelling of the induction motor for healthy and faulty motor has been discussedin the next section step by step.

The voltage equations in machine variables may be expressed by the following equations 1 and 2:

$$V_{abcs} = r_s i_{abcs} + \frac{d}{dt}(\quad) \tag{1}$$

$$V_{abcs} = r_s i_{abcs} + \frac{d}{dt}(\quad) \tag{2}$$

$$abcr \quad r \; abcr \quad abcr$$

Where, $\square \square \frac{d}{dt}$

The flux linkages equations (3 and 4) are shown as follows:

$$\phi_{abcs} = L_s i_{abcs} + L_{sr} i_{abcr} \tag{3}$$

$$\phi_{abcr} = (L_{sr})^T i_{abcs} + L_r i_{abcr} \tag{4}$$

The q-axis and d-axis stator voltage equations may be written as:

$$V \; \square \; r \, i \; \square\square\square \; \square \; \frac{\square}{\square} \; qs \tag{5}$$
$$\square \; qs \quad s \; qs \quad ds \quad b$$

Where, $\omega \; \square \frac{\square_s}{\omega_b}$

$$V \; \square \; r \, i \; \square\square\square \; \square \; \frac{\square}{\square} \; ds \tag{6}$$
$$\square \; ds \quad s \; ds \quad qs \quad b$$

$$V_{0s} = r_s i_{0s} + \frac{\square}{\omega_b} \Psi \tag{7}$$
$$0s$$

The q-axis and d-axis rotor voltage equations may be written as:

$$V \; \square \; r \, i \; \square\square\square \; \square \; \frac{\square}{\square} \; qr \tag{8}$$
$$\square \; qr \quad r \; qr \quad dr \quad b$$

Where, $\square \frac{\square_s \square \square_r}{\omega_b}$
$\square$

$$V \; \square \; r \, i \; \square\square\square \; \square \; \frac{\square}{\square} \; dr \tag{9}$$
$$\square \; dr \quad r \; dr \quad qr \quad b$$

$$V \; \square \; r \, i \; \square \; \frac{\square}{\omega} \; \square$$

(10)

$$0r \quad r \; 0r$$
$$0$$
$$rb$$

Where, $\omega = \frac{\omega_r}{\omega_b}$, ω_b =base speed

The developed electromagnetic torque in the motor is as shown in equation 11.

$$T_e = 1.5\frac{P}{2}\left(\frac{1}{\omega_b}\right)(\psi_{ds} i_{qs} - \psi_{qs} i_{ds}) \quad (11)$$

Where, P is the No. of poles of the motor.
The mechanical equation of the motor may be written as:

$$T_e - T_L - T_f = 2Hp\left(\frac{\omega_r}{\omega_b}\right) \quad (12)$$

Where H is the inertia constant, T_L is load torque and T_f is frictional torque of the motor

$$H = 0.5\left(\frac{2\pi}{P}\right)^2 \frac{J}{P_b} \quad (13)$$

Where, P_b is the base power of the motor.
The equations (1 to 13) give complete mathematical modelling of the used induction motor.

2.2 Modelling of stator inter-turn faulty condition of the motor

When inter-turn fault occur then the faulty phase is split into two sub windings located along the same magnetic axis. The equations (14) to (26) represent the final voltage equations for the stator and rotor windings, as well as the short-circuit current and the electromagnetic torque developed by the motor.

$$V_{qs} = V_{qs} - r_s i_{qs} - \omega_b \Psi_{ds} - \frac{p}{\omega_b} \Psi_{qs} \quad (14)$$

$$V_{ds} = V_{ds} - r_s i_{ds} + \omega_b \Psi_{qs} - \frac{p}{\omega_b} \Psi_{ds} \quad (15)$$

$$V_{0s} + \Delta V_{0s} = r_s i_{0s} + \frac{p}{\omega_b} \Psi_{0s} \quad (16)$$

$$V_{qr} = V_{qr} - r_r i_{qr} - \omega_b \Psi_{dr} - \frac{p}{\omega_b} \Psi_{qr} \quad (17)$$

$$V_{dr} = V_{dr} - r_r i_{dr} + \omega_b \Psi_{qr} - \frac{p}{\omega_b} \Psi_{dr} \quad (18)$$

$$V_{0r} = r_r i_{0r} + \frac{p}{\omega_{rb}} \Psi_0 \quad (19)$$

Where,

$$\frac{dV_{fs}}{dt} = \frac{n}{3}(2nL_{ls} - 3L_{ms})\cos\left(\frac{n}{3}\right) + \frac{n}{3} 2r_s \cos\left(\frac{n}{3}\right) \quad (20)$$

$$\frac{d}{dt}\lambda_{fs} = \frac{n}{3}(2nL_{ls} - 3L_{ms})\sin\theta_s - \frac{n}{3}i_f 2r_s \sin\theta_s \quad (21)$$

$$V_{0s} = \frac{n}{3}L_{ls}\frac{di_f}{dt} + \frac{k}{3}r_s i_f \quad (22)$$

and

$$V_{qr} = nL_{ms}(\cos\theta_s \frac{di_f}{dt} - \sin\theta_s i_f) \quad (23)$$

$$V_{dr} = nL_{ms}(-\sin\theta_s \frac{di_f}{dt} - \cos\theta_s i_f) \quad (24)$$

The fault intensity may be denoted as „n" and i_f is the fault current.

$$\begin{aligned} & n^2(L_{ls}+L_{ms})\frac{d}{dt}i_{fs}+(r_f+nr_s)i_{fs}+nr_s(i_{qs}\cos\theta_s+i_{ds}\sin\theta_s+i_{0s}) \\ & n(nL_{ls}+L_M)(-i_{qs}\sin\theta_s+i_{ds}\cos\theta_s)+n(nL_{ls}+L_M)\cos\theta_s\frac{di_{qs}}{dt}\sin\theta_s+i_{ds}\cos\theta_s\frac{di_{ds}}{dt} \\ & -n^2L_{ls}\frac{di_{0s}}{dt}=nL_M(i_{qs}\sin\theta_s+i_{ds}\cos\theta_s)+nL_M(\cos\theta_s\frac{di_{qr}}{dt}+\sin\theta_s\frac{di_{dr}}{dt}) \end{aligned} \quad (25)$$

The electromagnetic torque may be expressed as:

$$T_e=1.5\frac{P}{2}\frac{1}{\omega_b}(i_{ds}i_{qs}-i_{qs}i_{ds})=nL_M(i_{qs}\cos\theta_s-i_{ds}\sin\theta_s)(i_{fs}+i_{qr}+i_{ds}) \quad (26)$$

The equations (14 to 26) give the complete mathematical modelling of the faulty stator condition.

3. PROPOSED MODEL OF THE PWM INVERTER FED INDUCTION MOTOR

The force-commutated electronic switches such as IGBTs, MOSFETs and GTOs are used to achieve variable speed control in AC electrical machines. Nowadays, the Induction motor fed by PWM inverter Voltage Sourced Converter (VSC) is replacing DC motors and Thyrister bridges gradually. In this paper, the use of the IGBT inverter fed into squirrel cage induction motor has been discussed. The IGBT inverters are having superior characteristics over other power electronics semiconductor based inverters in many power electronics & drives applications. Therefore, in the present section, an induction motor fed PWM inverter model with IGBT inverter has been implemented in the recent Matlab/Simulink environment.

A three-phase squirrel cage induction motor having rating of 3 HP, 220 V, 1430 RPM is fed by a PWM inverter which has been considered and shown in Figure 1. The base frequency of the sinusoidal reference wave is 50 Hz, whereas the triangular carrier wave's frequency is set to 1650 Hz. it corresponds to a frequency modulation factor m of 33(50Hz×33=1650 Hz). The maximum time step has been limited to 10 μs, it is needed due to the relatively high switching frequency (1650 Hz) of the inverter. It is recommended that m_f should be an odd multiple of three and that the value ought to be as high as possible [21].

The induction machine's rotor is short-circuited for Squirrel Cage Induction Motor. Its stator leakage inductance is set to twice from its actual value to simulate the effect of a smoothing reactor placed between the inverter and the induction motor. The motor is started from standstill condition. The speed set point is set to 1430 RPM under full load condition. This speed is reached after 0.3 s and it has been observed that the stator and rotor currents are quite "noisy," in spite of the use of a smoothing reactor. The noise introduced by the PWM inverter has also been observed in the electromagnetic torque waveform Te, though the motor's inertia prevents this noise from appearing in the motor's speed waveform.

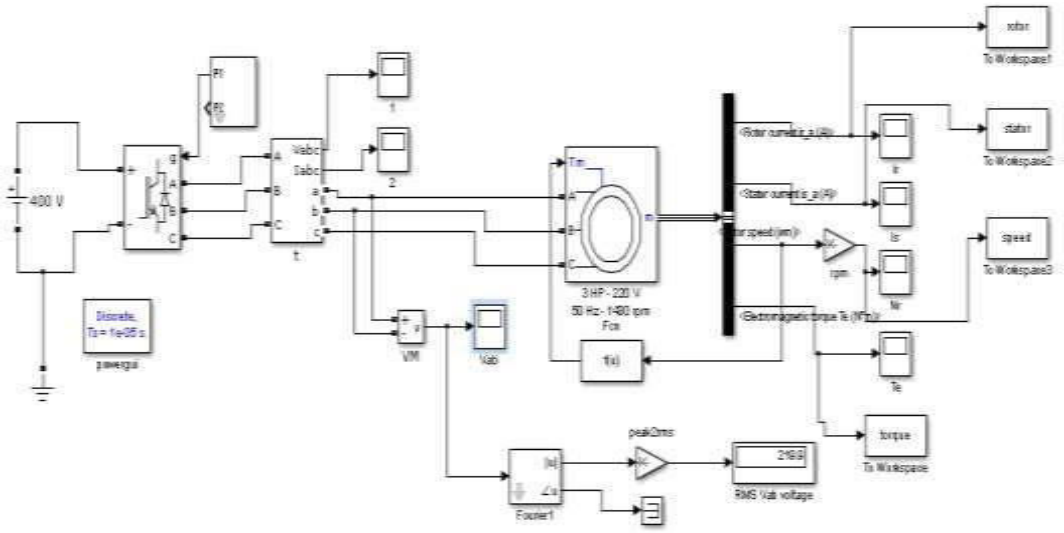

Figure 1. PWM inverter fed induction motor simulation model

The reference frame is used to convert input voltages (abc reference frame) to the dq reference frame, and output currents (dq reference frame) to the abc reference frame. we may choose among the following reference frame transformations.

(i) Rotor reference frame (Park transformation)
(ii) Stationary reference frame (Clarke or αβ transformation)
(iii) Synchronous reference frame

The following instructions have been suggested by Krause &Thomas [21].

(i) Choose the stationary reference frame if the stator voltages are either unbalanced or dis-continuous andthe rotor voltages are balanced (or 0).
(ii) Choose the rotor reference frame if the rotor voltages are either unbalanced or discontinuous and thestator voltages are balanced.
(iii) Choose either the stationary or synchronous reference frames if all voltages are balanced andcontinuous.

For the stationary reference frame, the value of rotor angle is set to 0 and the value of β is set to $-\theta_r$. The choice of reference frame influenced the waveforms of all dq variables. It also influenced the simulation speed and in definite cases, the accuracy of the results.

In the present work, we may choose either stationary or synchronous reference frame. It has been observed that the synchronous or stationary reference frame gives approximately same results. Therefore, with this proposed model, either stationary or synchronous reference frame can be chosen.

The proficient and frequent method is used for producing the PWM pulses. For producing the PWM pulses comparison of the output voltage to synthesize (50 Hz in this case) with a triangular carrier's wave at the switching frequency 1650 Hz (in this case) is done. This method is employed in the Discrete 3- phase PWM pulse generator block in the Matlab/Simulink. The line-to-line RMS output voltage is a function of the DC input voltage and of the modulation index m as given in the following equation.

$$V_{LLrms} = \frac{m}{2}\sqrt{\frac{3}{2}}V_{dc} = 0.612\,m\,V_{dc} \qquad (27)$$

Therefore, a DC voltage of 400 V with a modulation factor of 0.90 yields the 220 V RMS voltages, which isthe nominal voltage of the used induction motor.

The fundamental component (50 Hz) is computed by the discrete Fourier block which is embedded inthe chopped V_{ab} voltage and in the phase a current.

Simulation results of the healthy condition of the motor under full-load

The simulation results in healthy or symmetrical motor condition of the induction motor are as shown in Figure 2. Totally four motor parameters have been considered for the analysis of the IM. These parameters are stator current, rotor current, rotor speed and developed electromagnetic torque. Two healthy modes have been considered; First healthy mode is for standstill condition and second is for runningcondition, since we are focusing on transient analysis of the motor. Therefore, we also need to observe how motor is behaving in the running conditions. Firstly, for healthy mode of the motor, the slip is set at 1(s=1) with nominal mechanical load torque 15 N-m. Secondly, for running condition, the slip is set at 0.04 with same load torque and may be observed from Table 1 and Table 2.

Theses tables reveal the changes in motor parameters in transient conditions for healthy as well as for stator inter-turn fault of the motor.

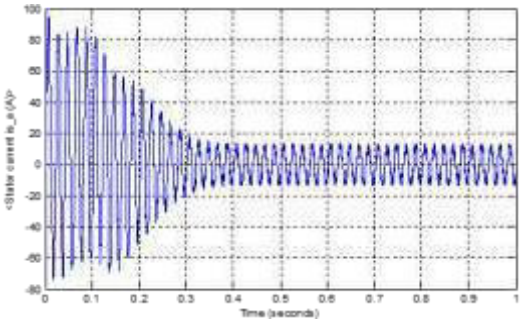

(a)

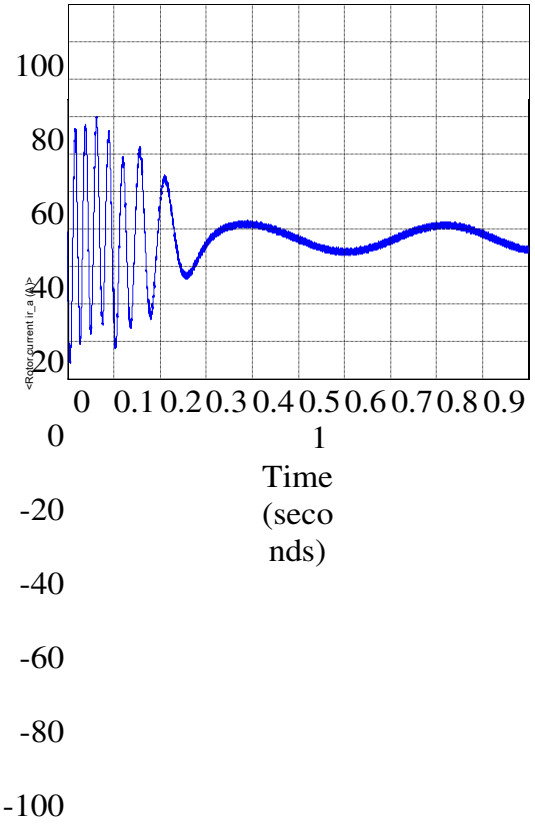

(b)

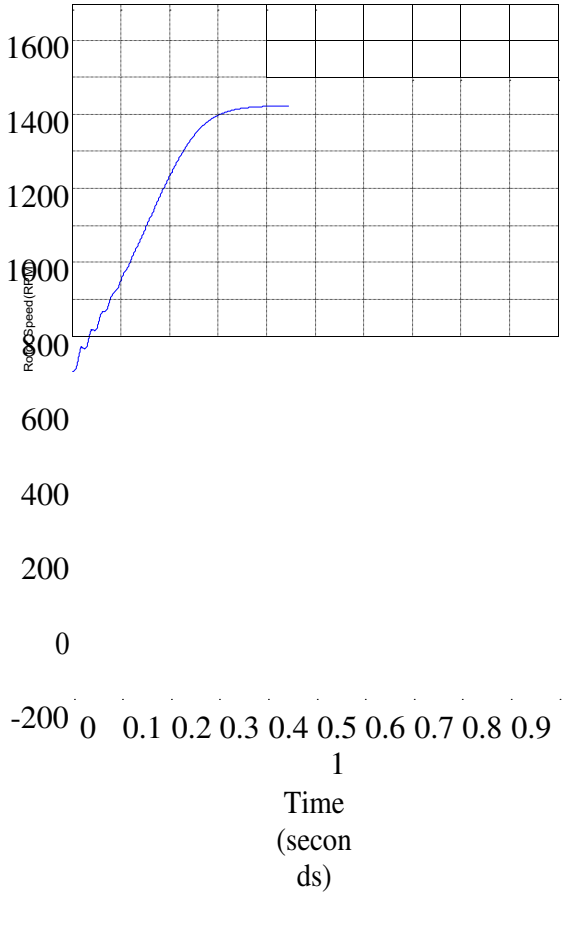

(c)

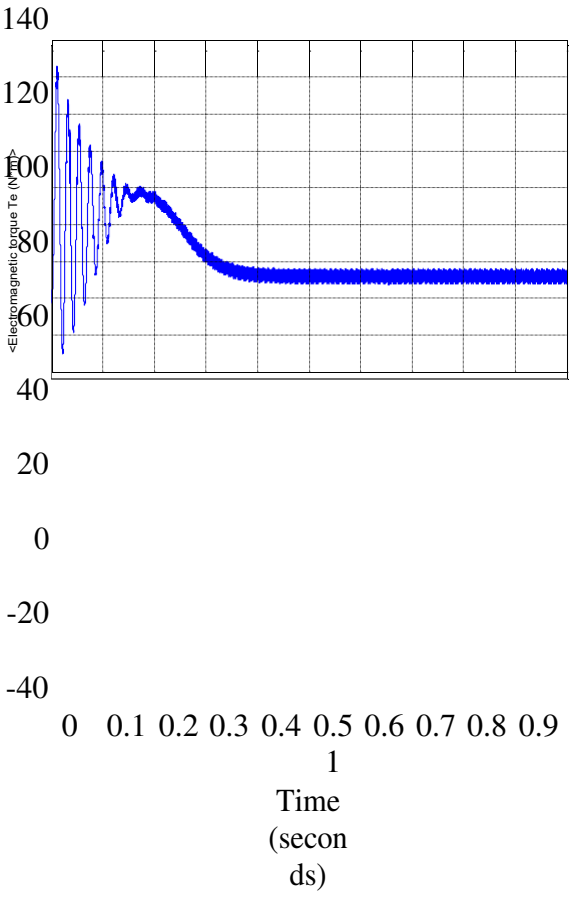

(d)

Figure 2. Results in healthy condition at full-load, (a) Stator current, (b) Rotor current, (c) Rotor speed,
(d)Electromagnetic torques

Table 1. Motor Signatures Variation for Healthy and Faulty Conditions of the Im at Full-Load

MC	LT (N-m)	Slip	DCV (V)	MPTSC (A)	MPTRC (A)	RS (RPM)	MPTEMT (N-m)	Vab (rms)
H-Y	15	1	400	95.46	87.12	1430 (RMF)	128.17	219.9
H-Y-F-L	15	0.04	400	86.76	79.80	1430	54.06	219.9
SITF	15	0.08	460	98.45	87.09	1380	81.92	252.9
SITF	15	0.08	470	100.58	88.95	1380	85.91	258.4

Table 2. Motor Signatures Variation for Healthy and Faulty Conditions of the Im at No-load

MC	LT (N-m)	Slip	DCV (V)	MPTSC (A)	MPTRC (A)	RS (RPM)	MPTEMT (N-m)	Vab (rms)

H-Y	0	1	400	95.46	87.20	1500 (RMF)	128.17	219.9
H-Y-F-L	0	0.04	400	86.97	80.33	1500	50.28	219.9
SLF	0	0.01	460	101.20	95.17	1485	63.50	252.9
SLF	0	0.01	470	103.21	97.22	1485	67.12	258.9

The obtained results in Figure 2 show that, all the considered motor parameters have reached in the steady state condition after 0.3 seconds. If we change the physical parameters of the motor used in the proposed model, such as slip and input voltage, then the healthy IM motor is treated like as faulty stator inter-turn of IM. If we increase input voltage above the prescribed limit, the overheating will occur and the insulation may get damage. As a result, stator inter-turn fault will be taken place. Causing this, the motor will reach in the idle condition for long periods. The model has been simulated only for 1s for clear revelation of the transient characteristics of the motor. Since this is a non-intrusive technique, the obtained simulation results for healthy as well as faulty conditions of the motor ought to be different. As a result, an effective stator inter-turn analysis would be carried out. From this model, the stator inter-turn fault would be diagnosed for full-load, half-load and no-load conditions.

Simulation results of the faulty inter-turn condition of the motor under full-load for DC voltage 460V

The healthy IM has been treated as the faulty IM in the Matlab/Simulink environment, if we varied some physical parameters such as input voltage as well as slip. In this paper, stator inter-turn fault analysis has been carried out in time domain only for input voltage 460 V and 470V. The obtained results for input voltage 460 V have been compared with the results of healthy condition. After observing waveforms of healthy and stator inter-turn faulty motor in Figure 2 and Figure 3, it may be concluded that the obtained results are different. Because it is a non-intrusive technique, we may consider that efficient stator inter-turn fault detection has been carried out in the time domain analysis.

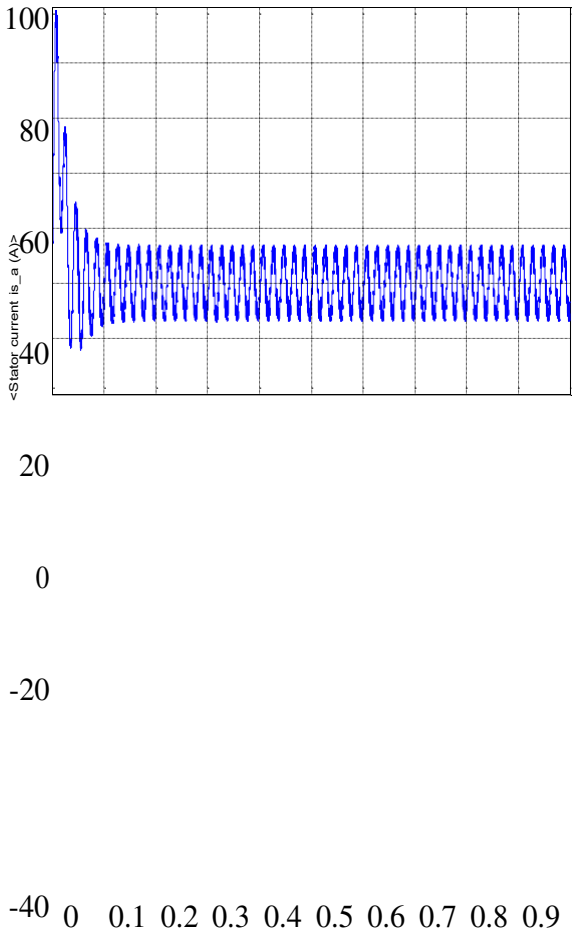
100
80
60
40
20
0
-20
-40
<Stator current is_a (A)>
0 0.1 0.2 0.3 0.4 0.5 0.6 0.7 0.8 0.9 1
Time (seconds)

(a)

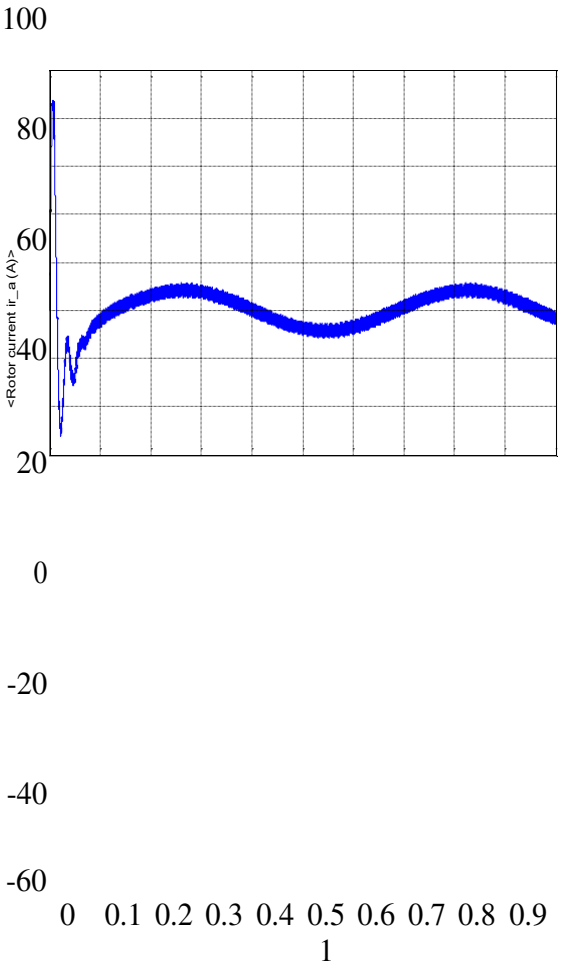
100
80
60
40
20
0
-20
-40
-60
<Rotor current ir_a (A)>
0 0.1 0.2 0.3 0.4 0.5 0.6 0.7 0.8 0.9 1
Time (seconds)

(b)

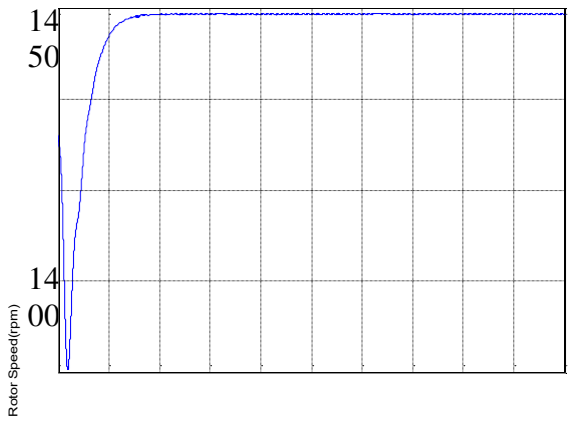
1450
1400
Rotor Speed(rpm)
1350
1300

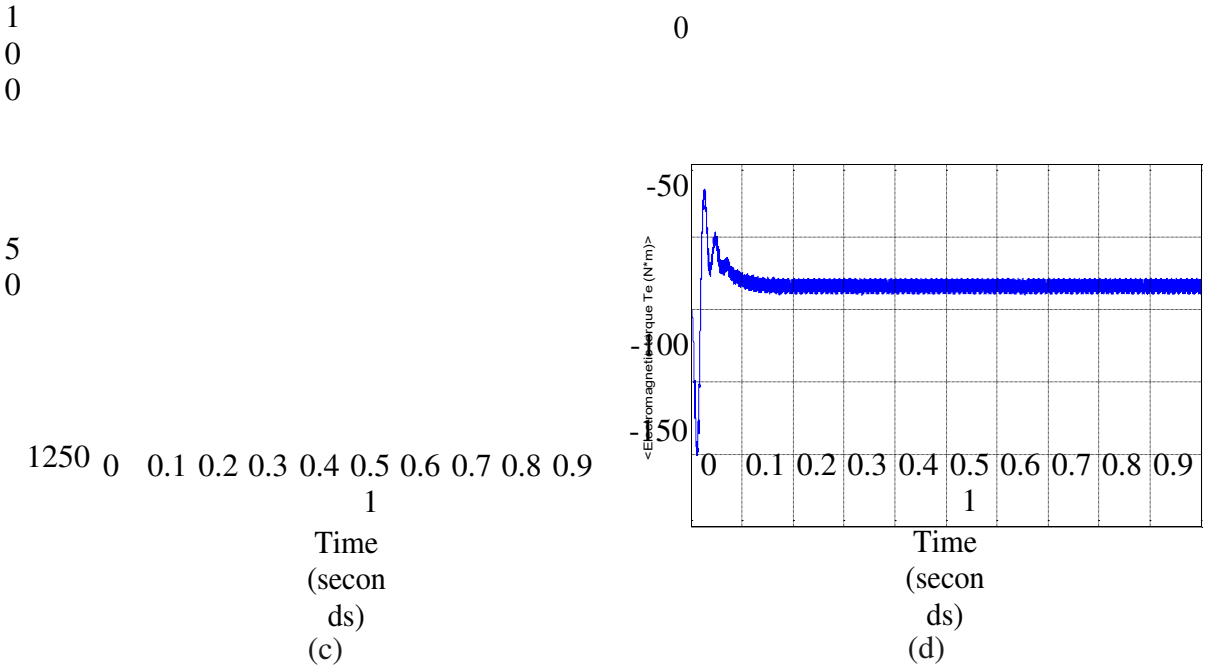

Figure 3. Results in faulty stator inter-turn condition at full-load, (a) Stator current, (b) Rotor current, (c)Rotor speed, (d) Electromagnetic torques

From Figure 3(a to d), it may be clearly observed that the transient state of the motor is completely disturbed and corresponding changes in motor parameters are as shown in Table 1 for healthy and faulty stator inter-turn. The motor signatures variation for both healthy and faulty inter-turn conditions of the induction motor for full load in Tabular form has been shown in the Table 1.

The rotor speed variation for input voltage 470 V for full-load condition is as shown in Figure 4. The rotor speed waveforms are as shown in Figure 3(c) and Figure 4. From both these Figureures, it has clearly been observed that the first maximum transient peak speed is 1380 rpm for both input voltage (460 V and 470V). But, if we observe the steady state responses of rotor speed shown in Figure 3(c) and Figure 4, it may be clearly observed that if the input voltage increases, the losses may get increased and consequently THD increased. Therefore, heating will occur. As a result, stator fault may take place. Now again observe the steady state response of Figure 3(c) and Figure 4, Indeed, the steady state rotor speed attains same value but losses are more because more distortion visualized in the Figure 4 steady state response.

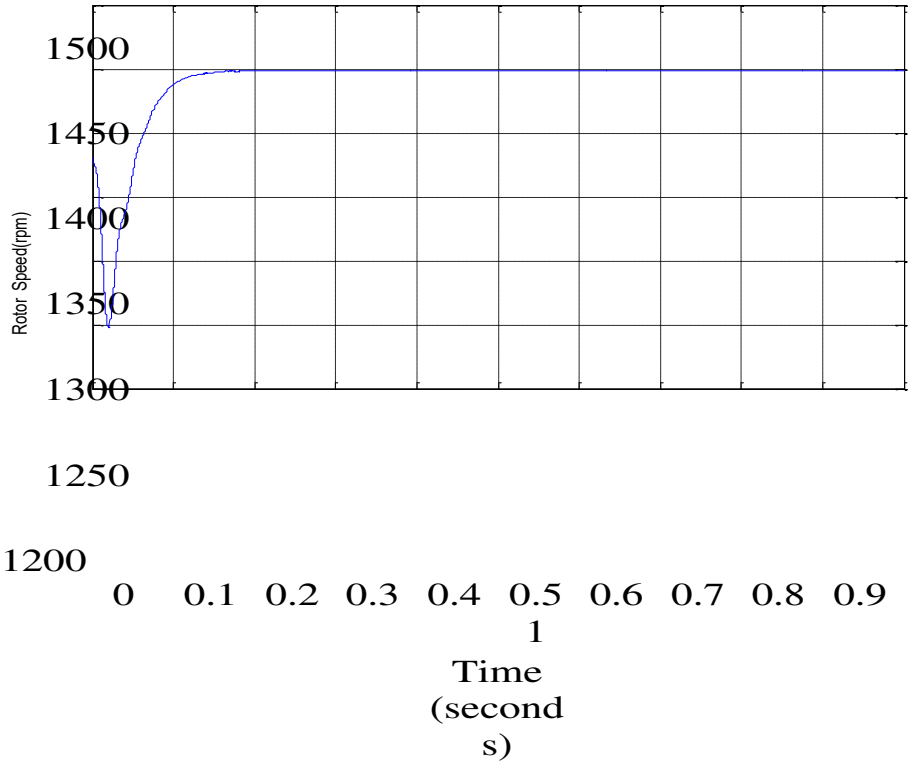

Figure 4. Rotor speed at full-load for input voltage 470 V

The nominal load torque is kept constant i.e. 15 N-m. The analysis has been carried out for healthy condition of the motor when slip is set at 1 and other healthy running condition of the motor for full load when slip is set at 0.04. The first maximum transient peak has been observed for both healthy and faulty inter-turn conditions of the motor. The input voltage under both healthy conditions is set at 400 V, the rotor is in standstill condition and the slip is set at 1, consequently, the speed of the Rotating Magnetic Field (RMF) reached the steady state condition after 0.3 sec up to 1430 rpm. In this case, the rotor speed is observed to be zero as shown in Figure 2(c). In this case, the motor speed reached 1430 rpm speed that is our rated speed of the motor. This condition has been achieved when nominal input voltage given for the machine. Now, we changed the input voltage keeping the load torque being the same. The healthy motor will be treated as stator inter-turn faulty motor. The increase in voltage overheated the motor so that consequently, the motor will achieve the idle condition for long periods.

In the present section, the stator inter-turn fault analysis has been done for full load conditions for input voltage 460V and 470V. It has been again observed from Table 1 that, all the motor parameter's first transient peak is increased except electromagnetic torque. The first maximum peak

MC: motor condition, LT: load torque, DCV: DC input voltage, MPTSC: maximum peaktransient stator current, MPTRC: maximum peak transient rotor current, RS: rotor speed, MPTEMT: maximum peaktransient electromagnetic torque, SITF: stator inter-turn fault

Electromagnetic torque is getting increased in the faulty condition as compared to the obtained electromagnetic torque in both healthy conditions. Therefore, over heating may cause motor stator inter-turn failure and we can say that efficient stator inter-turn fault

detection has been completed for full load conditions in time domain by the proposed model.

Simulation results of the healthy condition of the motor under no-load

The results of healthy and stator inter-turn faulty conditions of the motor under no-load is as shown in Figure 5 and Figure 6. It has been observed from all the considered motor signatures which reached the steady state conditions after 0.3 s like full-load. But, if we compare the obtained values in no-load condition from values obtained in full load condition, they are different. For healthy no-load standstill condition, the RMF value is 1500 rpm. When the slip is set 0.04 for no-load running condition, the rotor speed has been obtained to be 1500 rpm. The corresponding changes in the motor signatures under no-load condition are as shown in Table 2. If we compare developed electromagnetic torque for healthy running condition in no-load from the full load running condition, it has been observed that the developed motor torque is more in full load condition rather than no-load condition unlike stator and rotor currents.

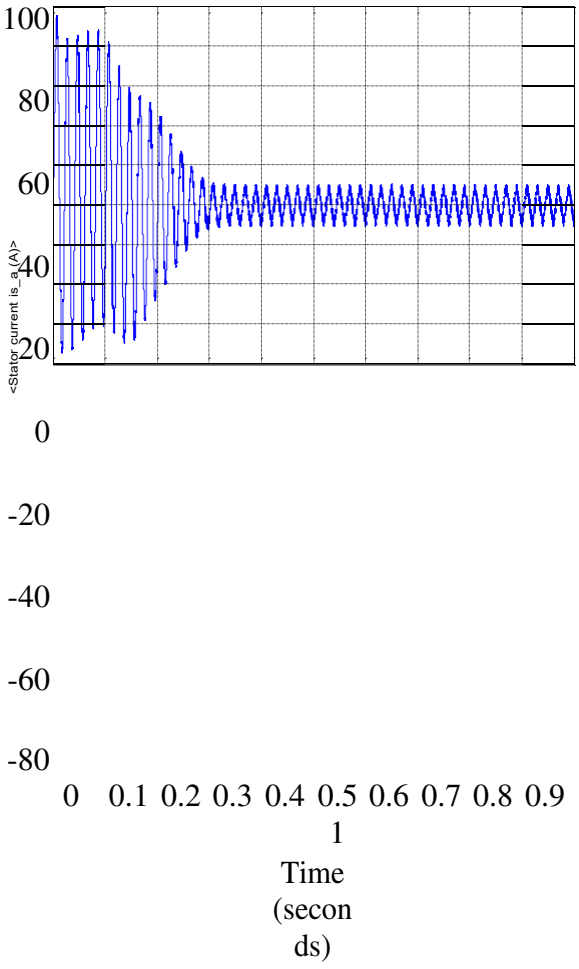
100
80
60
40
20
0
-20
-40
-60
-80
<Stator current is_a (A)>
0 0.1 0.2 0.3 0.4 0.5 0.6 0.7 0.8 0.9 1
Time (seconds)

(a)

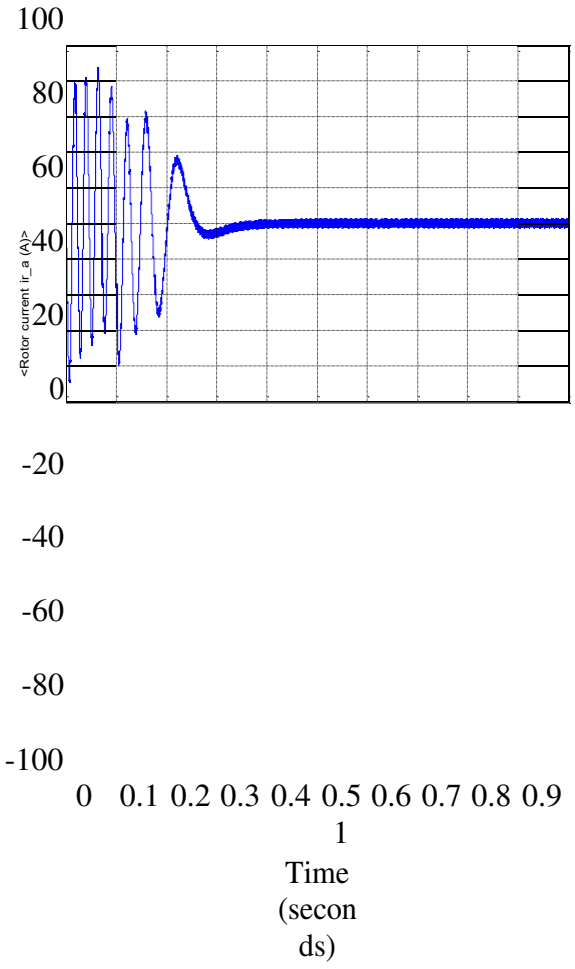
100
80
60
40
20
0
-20
-40
-60
-80
-100
<Rotor current ir_a (A)>
0 0.1 0.2 0.3 0.4 0.5 0.6 0.7 0.8 0.9 1
Time (seconds)

(b)

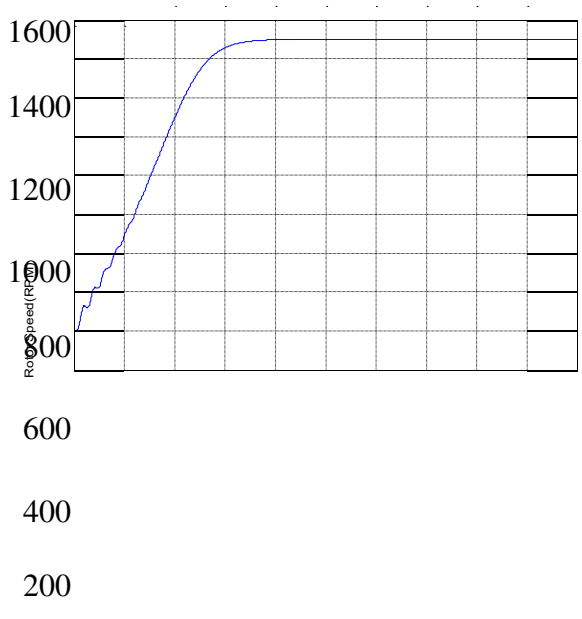
1600
1400
1200
1000
800
600
400
200
0
Rotor Speed(RPM)

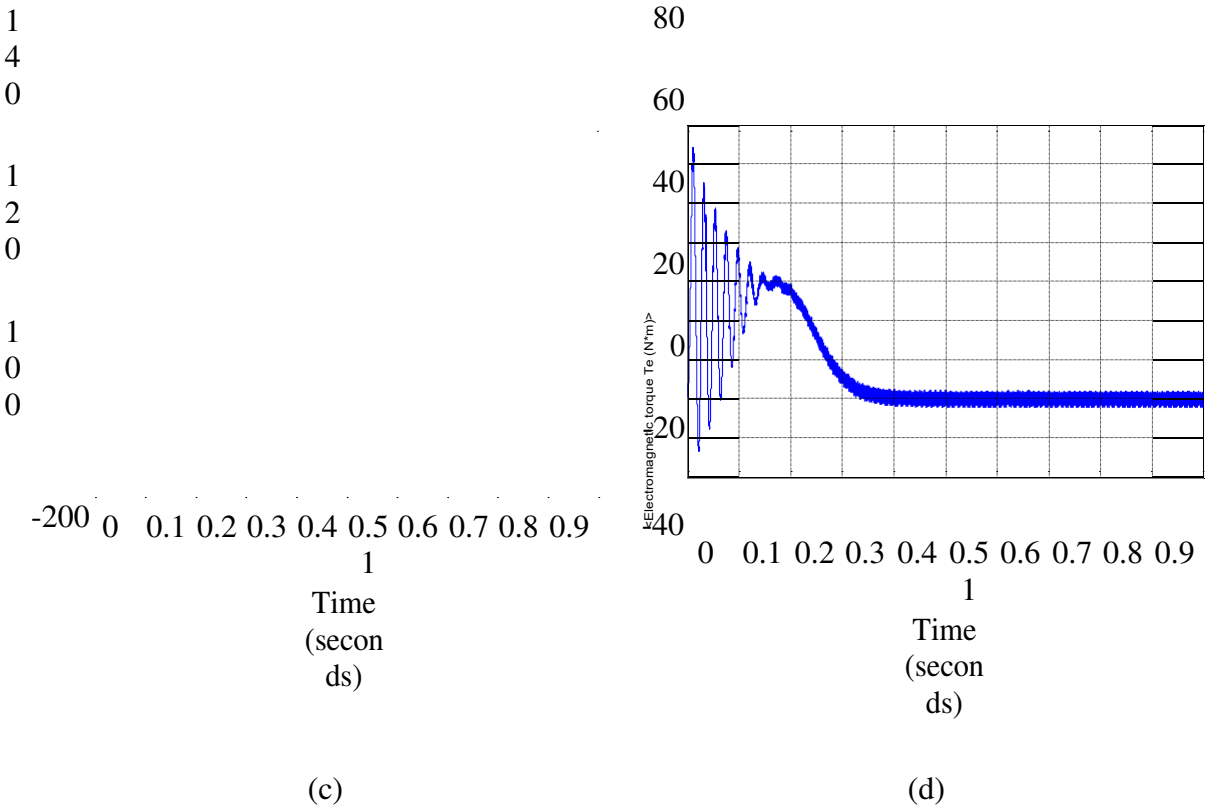

Figure 5. Results in healthy condition at no-load, (a) Stator current, (b) Rotor current, (c) Rotor speed, (d)Electromagnetic torques

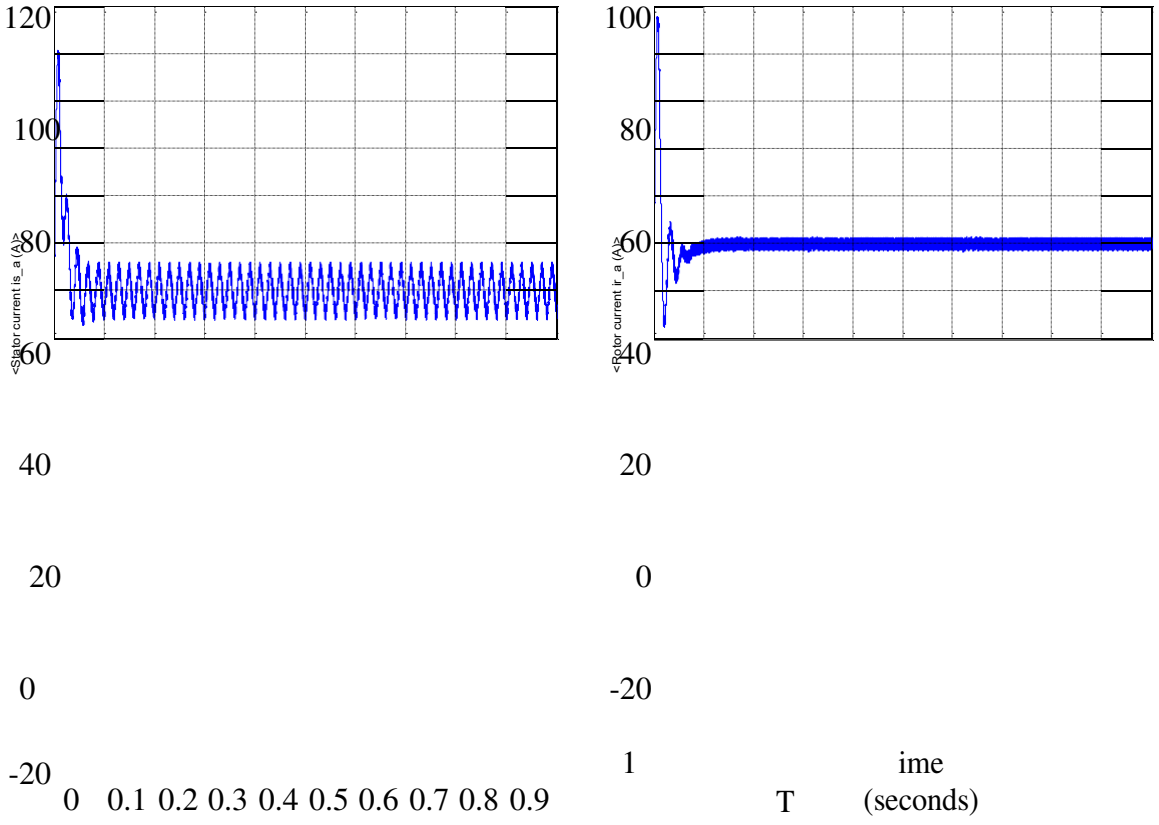

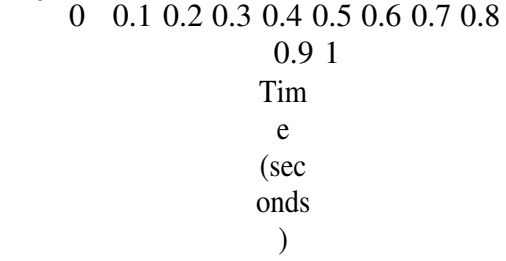

(a) (b)

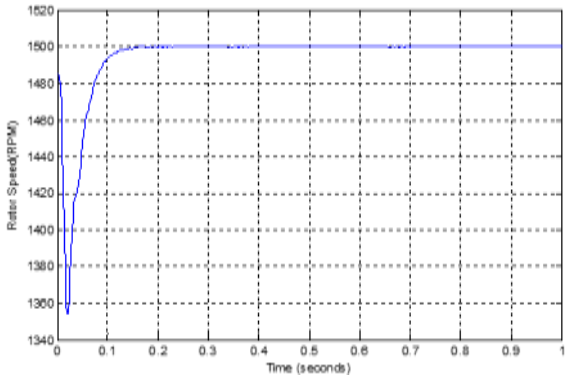

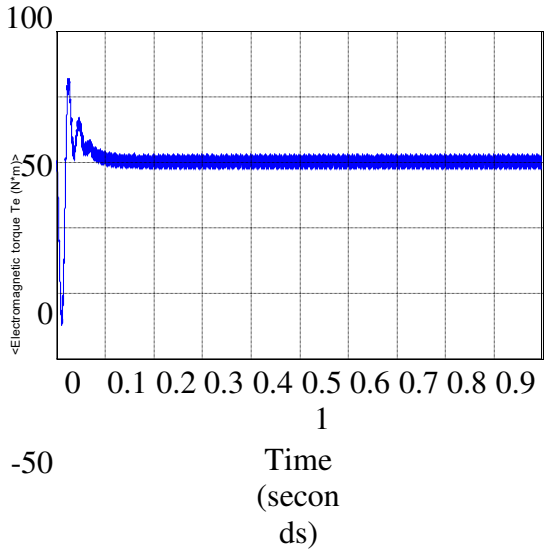

(c) (d)

Figure 6. Results in faulty stator inter-turn condition at no-load, (a) Stator current, (b) Rotor current, (c)Rotor speed, (d) Electromagnetic torques

Simulation results of the faulty inter-turn condition of the motor under no-load for DC voltage 460V

From Figure 6, it has clearly been observed that the transient state of the motor has completely been disturbed and correspondingly changes in motor signatures are as shown in Table 2 for stator inter-turn fault. The motor signatures variation for healthy and faulty stator inter-turn conditions of the induction motor for no-load has been clearly understood from Table 2. The nominal load torque is kept constant i.e. 0 N-m for no-load condition. The analysis has been carried out for healthy condition of the motor when slip is set at 1 and other healthy running condition of the motor for full load when slip is set at 0.04. The first maximum transient peak has been observed for healthy and faulty conditions of the motor. The input DC voltage in the healthy condition is set at 400V. When slip is set at 1, the rotor is in standstill condition and the motor speed reached the steady state condition after 0.3 sec upto 1500 rpm. Therefore, in the healthy running condition of the motor, the rotor speed is reached at 1500 rpm after 0.3 s. This condition has been achieved when there is no overvoltage applied on the machine.

Now, we increased input voltage and kept load torque constant i.e. 0 N-m under no-load condition. Appling this overvoltage i.e. 460 V or more than 460V. The safety factor of the stator winding insulation lost for the value of input voltage 460V or more. The healthy motor will be now treated as faulty motor. The increase in input voltage above the prescribed value will cause over heating of the motor. Consequently, it leads to stator inter-turn fault.

The inter-turn stator fault analysis has been done under no-load conditions for input voltage 460V and 470V. All the motor parameters‟ first transient peak is increased except electromagnetic torque. The first maximum peak electromagnetic torque is getting increased in the faulty condition as compared to the obtained electromagnetic torque in both healthy conditions. Therefore, efficient stator inter-turn fault detection has been done under no-load conditions in time domain.

The rotor speed waveforms for no-load condition are as shown in Figure 6(c) and Figure 7 for input voltage 460 V and 470 V respectively. It has been observed that the first maximum peak transient rotor speed is same for voltage 460 V and 470 V i.e. 1485 rpm, but if we observe steady state response which has been taken place after 0.1 s, the waveforms clearly show that the increase in input voltage results more losses and rise in total harmonic distortion (THD). As a result, more heating will take place and failures the winding.

Since, this is a non-intrusive technique of the fault detection. Therefore, the results obtained in the transient condition for healthy as well as faulty condition ought to be different. We have obtained expected results. Therefore, we may conclude that efficient stator inter-turn fault detection has been taken place by proposed model with time domain analysis.

The transient variation in the motor signatures in healthy condition is as shown in Table 3. It has been observed from the Table 3, the considered motor signatures are varying with the input voltage. It has

Table 3. Motor Signatures Variation with Dc Input Voltage in Healthy Condition

Load Torque (N-m)	Input DC Voltage (V)	MPTSC (A)	MPTRC (A)	RS (RPM)	TEMT (N-m)	V_{ab} (RMS)
15	400	95.66	86.17	1430	129.26	219.9
15	420	100.43	90.55	1437	142.13	230.9
15	440	105.20	94.69	1442	155.58	241.9
15	450	107.58	97.21	1445	162.52	247.4

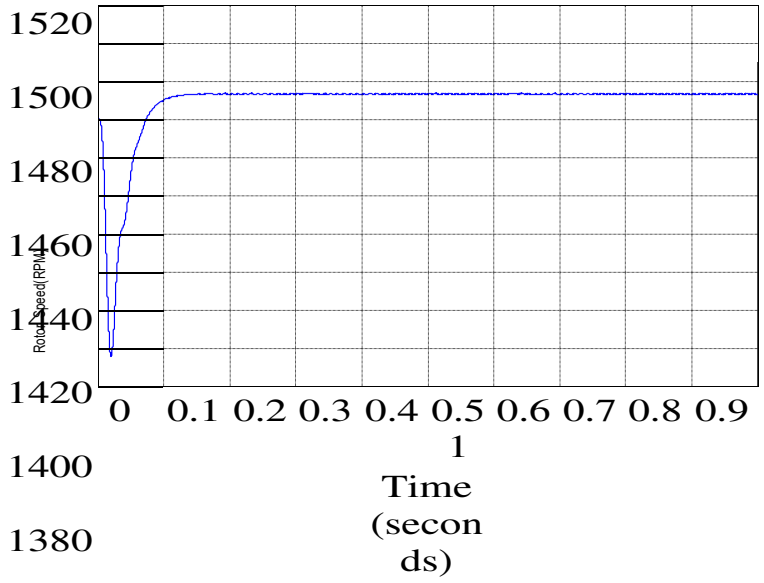

Figure 7. Rotor speed at no-load for input voltage 470 V

Clearly been observed that if we increase input DC voltage equal or above 260 V then the safety factor of the insulation exceeded. Therefore, the overvoltage withstand capability has lost and insulation failure consequently, stator winding will be broken down. In this analysis, the stator inter-turn fault created when input DC voltage V_{in} (DC) = V_{in}(DC) + 60 and V_{in}(DC) = V_{in}(DC) +70 . The calculated overvoltage has been applied for creating stator-inter-turn fault. Where, V_{in} (DC) is input applied DC voltage.

Therefore, we may say that by this model stator inter-turn fault has been diagnosed efficiently in the transient condition. Further, the stator current motor parameter has been used for stator inter-turn fault diagnosis purpose for all load conditions. The results of healthy and faulty condition of the motor for full load, half-load and no-load is as shown in Figure 8. Due to non-intrusive nature of waveforms, among the figure are different from each

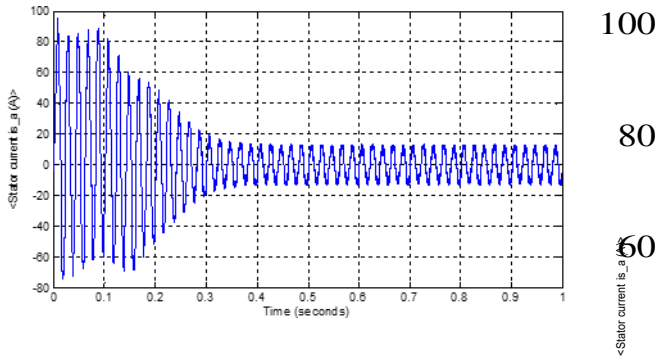

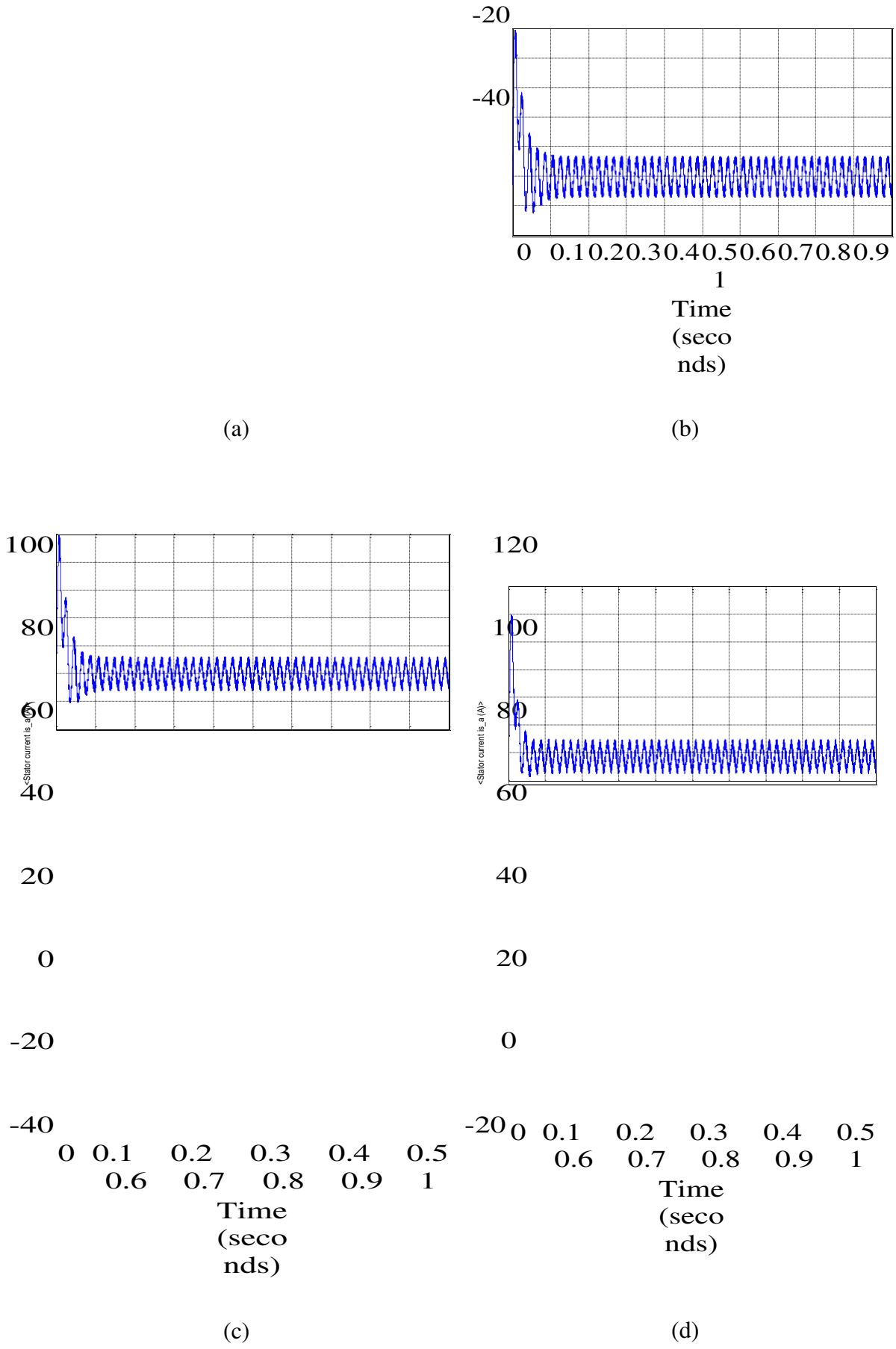

Figure 8. Results in healthy and faulty stator inter-turn condition various loads, (a) Healthy stator current, (b)Faulty stator current at full-load, (c) Faulty stator current at half-load,

(d) Faulty stator current at no-load

Other therefore, we may conclude that the Motor Current Signature Analysis (MCSA) technique can be used for stator fault diagnosis purpose for all load conditions. It is also noticed that, the diagnosis of any fault by time domain technique is a very tedious task and many faults are not visible by this method. Therefore, for accurate fault diagnosis purpose, the FFT and Wavelet Transform for frequency and time- frequency information might be used in future.

4. CONCLUSIONS

In the present paper, the squirrel cage induction motor fed PWM inverter model with direct torque control jointly has been proposed and developed in the recent Matlab/Simulink environment. The proposed simulation model has been used to diagnose incipient stator inter-turn fault of the squirrel cage induction motor in time domain analysis. The time domain analysis technique has been used to diagnose stator inter- turn fault for various loads in the transient condition. The main aim of this research paper is to create stator fault in the proposed simulation model and their analysis in time domain, when motor is running in the full- load conditions. In the past, it has been widely observed that the FFT algorithm based technique only work for constant load conditions. The obtained simulation results show that the waveforms of healthy and faulty stator conditions are completely dissimilar to each other. It has also been noticed that the detection of stator inter-turn fault by time domain analysis is a tedious process but major information are hidden in the form of frequency. The time domain analysis cannot determine at what time which frequency exist. Finally, we may conclude that for other induction motor faults MCSA is suitable but also for stator fault at varying load condition, the use of advanced DSP based transformative techniques such as FFT or WT should be preferred. The proposed model may be used in various power electronics and drives applications.

REFERENCES

[1] Khadim Moin Siddiqui, Kuldeep Sahay, V. K. Giri, "Simulation And Transient Analysis of PWM Inverter Fed Squirrel Cage Induction Motor Drives," *i-manager's Journal on Electrical Engineering*, vol. 7, no.3, pp.9-19, Jan- March 2014.

[2] K.M. Siddiqui et.al., "Health Monitoring and Fault Diagnosis in Induction Motor- A Review," *International Journal of Advanced Research in Electrical, Electronics and Instrumentation Engineering*, vol. 3, No. 1, pp. 6549- 6565, 2014.

[3] Khadim Moin Siddiqui and V. K. Giri, "Broken rotor bar fault detection in induction motors using Wavelet Transform," *2012 International Conference on Computing, Electronics and Electrical Technologies (ICCEET)*, Kumaracoil, 2012, pp. 1-6.

[4] J. CusidÓCusido, L. Romeral, J. A. Ortega, J. A. Rosero and A. GarcÍaGarcia Espinosa, "Fault Detection in Induction Machines Using Power Spectral Density in Wavelet Decomposition," in *IEEE Transactions on Industrial Electronics*, vol. 55, no. 2, pp. 633-643, Feb. 2008.

[5] A. Stavrou, H. G. Sedding and J. Penman, "Current monitoring for detecting inter-turn short circuits in induction motors," in *IEEE Transactions on Energy Conversion*, vol. 16, no. 1, pp. 32-37, March 2001.

[6] Jagadanand G. et.al., "Inter-turn Fault Detection in Induction Motor using Stator Current Wavelet Decompsition," *International Journal of Electrical Engineering & Technology*, vol.3, no.2, pp.103-122, July-Sept. 2012.

[7] O. Duque-Perez, D. Morinigo-Sotelo and M. Perez-Alonso, "Diagnosis of induction motors fed by supplies with high harmonic content using motor current signature analysis," *2011 International Conference on Power Engineering, Energy and Electrical Drives*, Malaga, 2011, pp. 1-6.

[8] T. W. Chua, W. W. Tan, Z. Wang and C. S. Chang, "Hybrid time-frequency domain analysis for inverter-fed induction motor fault detection," *2010 IEEE International*

Symposium on Industrial Electronics, Bari, 2010, pp. 1633-1638.

[9] M. S. Ballal et.al, "Stator Winding Inter-turn Insulation Fault Detection in Induction Motors by Symmetrical Components Method," *Electric Power Components and Systems*, vol. 36, no. 7, pp.741–753, July 2008.

[10] A. H. Bonnett and G. C. Soukup, "Cause and analysis of stator and rotor failures in three-phase squirrel-cage induction motors," in *IEEE Transactions on Industry Applications*, vol. 28, no. 4, pp. 921-937, July-Aug. 1992.

[11] T. A. Kawady et.al., "Modeling and Experimental Investigation of Stator Winding Faults in Induction Motors," *Electric Power Components and Systems*, vol. 33, pp.599-611, Oct 2008.

[12] L. Frosini, E. Bassi and L. Girometta, "Detection of stator short circuits in inverter-fed induction motors," *IECON 2012 - 38th Annual Conference on IEEE Industrial Electronics Society*, Montreal, QC, 2012, pp. 5102-5107.

[13] B.Liang et.al, "Simulation And Fault Detection of Three-Phase Induction Motors," *Journal in Mathematics and Computers in Simulation,* vol.61, no. 1, pp.1-15*,* 2002.